Geotechnical Testing Journal, Vol. 28, No. 2
Paper ID GTJ12648
Available online at: www.astm.org

Mostafa A. Ismail,[1] *Shambhu S. Sharma,*[2] *and Martin Fahey*[3]

A Small True Triaxial Apparatus with Wave Velocity Measurement

ABSTRACT: This paper describes a new cubical, true triaxial apparatus recently developed at the University of Western Australia (UWA). The apparatus is a stand-alone unit of the rigid type, where three pairs of pistons can be pressurized to impose three independent, rectilinear stresses on a sample of 250 mm side length. The sample can be tested either dry or saturated. Both drained and undrained shearing can be carried out with maximum pressure of about 1.5 MPa and maximum linear strain of about 8 % in any of the three principal directions. A wave velocity measurement system is incorporated so that both elastic shear (V_s) and compression (V_p) wave velocities can be measured, with the wave travelling between any two opposite faces of the device, or along skew paths. The elastic waves are generated and detected using "in house" manufactured wave transducers, which can access the sample externally. This feature enables the shear transducers to be rotated 90° degrees to change the polarization direction, enabling V_s to be measured in inclined planes. Additionally, the device enables accurate measurement of K_o. The paper presents results obtained from a silica sand to show the capability of the new device.

KEYWORDS: true triaxial, small-strain stiffness, shear and compression wave velocity, silica sand, piezoelectricity

Introduction

Accurate evaluation of shear (V_s) and compression (V_p) wave velocities of geomaterials is becoming an indispensable exercise in many geotechnical applications, both in the field and the laboratory. These velocities can be used to calculate the small-strain shear modulus (G_o) and constrained modulus (M_o), respectively, through the following relationships

$$G_o = V_s^2 \, \rho \tag{1}$$

$$M_o = V_p^2 \, \rho \tag{2}$$

where ρ is the bulk density of the tested material.

Loads from geotechnical structures usually induce complicated stress paths that may influence the small-strain moduli of soils. Investigation of such influence in the laboratory requires the ability to define completely (in terms of magnitude and direction) the three independent principal stresses acting on a soil element. The ability to control each of these stresses is also important during investigation of the influence of the maximum stress ratio ($R = \sigma'_1/\sigma'_3$) on G_o; values of $R \geq 2$ have been reported to reduce G_o by 20–30 % (Yu and Richart 1984).

Early work (Roesler 1979) on the influence of the principal stress components on G_o showed that it is the individual components of such stresses that affect the modulus rather than the mean effective stress, p'; hence, clear distinction between each of these components is essential in the course of investigating the small-strain behavior. Particularly, it is universally accepted that the normal stresses that affect G_o are those acting in the directions of particle motion (polarization) and wave propagation; therefore, the role of the intermediate principal stress cannot be ignored. As such, conventional triaxial apparatus (e.g., Pennington et al. 2001), resonant column device (e.g., Hardin and Drnevich 1972; Santamarina and Cascante 1996), where the horizontal radial stress is kept constant, 1-d consolidation cells (e.g., Zeng and Ni. 1999), or direct simple shear devices (Dyvik and Olsen 1989) have limited applications and cannot be used to investigate the effect of a general stress state on the small-strain modulus.

The limitations discussed above led researchers to either develop new devices for such purposes, or to incorporate S- and P-wave velocity measurement capability into the devices that can control each of the stress components mentioned above. Examples of such devices are the torsional hollow cylinder (Saada 1988; Nakamura et al. 1999) and the large-scale, true triaxial apparatus of Stokoe et al. (1985).

The studies involving measurement of V_s and V_p using the true triaxial device were reported to involve very large samples. For example, Stokoe et al. (1985) used a sample as large as 2.1 m side length. Obviously, working with large-scale devices of such size is very time-consuming, and the devices themselves may be expensive to construct and maintain. Although Roesler (1979) measured V_s under three independent principal stresses on a small cubic sample of 0.3 m, the loading regime was limited to a combination of isotropic (by vacuum) and vertical loading. This entailed rotation of the sample twice to control each of the principal stresses.

This paper describes a new, cost-effective, true triaxial apparatus of reasonable size ($0.25 \times 0.25 \times 0.25$ m) that can be used to control independently each of the three principal stresses while measuring V_s and V_p of a reconstituted soil sample (cemented or uncemented). Location of the shear and compression wave transducers allow the measurement to be carried out either along a rectilinear or a skew path. The paper presents results obtained on a silica sand, showing the excellent capabilities of the new apparatus.

Received May 12, 2004; accepted for publication August 11, 2004; published March 2005.

[1] Lecturer, Centre for Offshore Foundation Systems, The University of Western Australia, 6009, Crawley, WA, Australia. E-mail: mismail@cyllene.uwa.edu.au

[2] Research Associate, Centre for Offshore Foundation Systems, The University of Western Australia, 6009, Crawley, WA, Australia.

[3] Professor, Centre for Offshore Foundation Systems, The University of Western Australia, 6009, Crawley, WA, Australia.

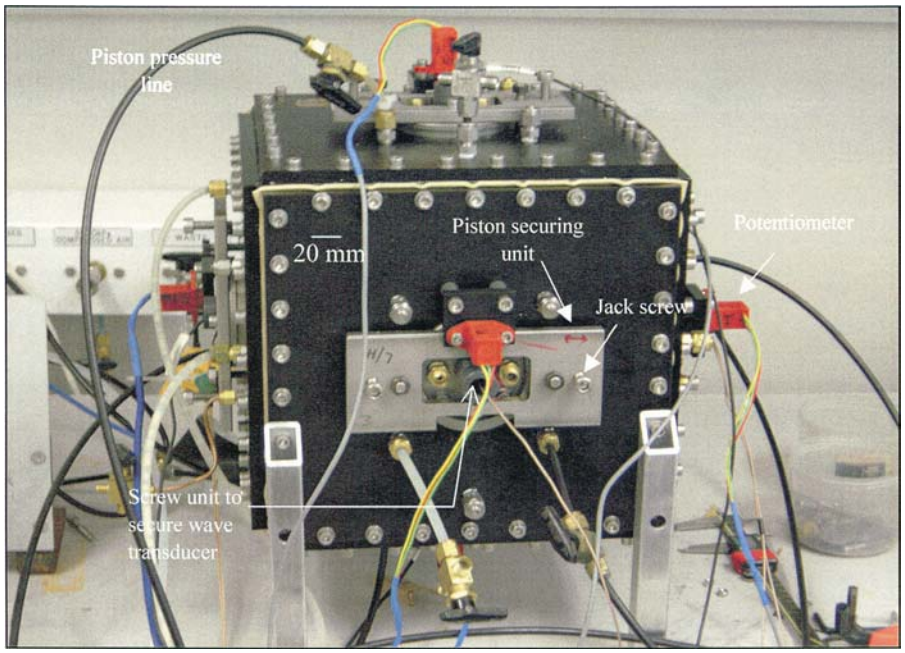

FIG. 1—*The true triaxial apparatus with wave velocity measurement transducers and pressurizing tubes.*

The New True Triaxial Device

The apparatus (Fig. 1) is made of anodized aluminum and comprises six pairs of square pistons mounted in a cubical frame of 250 mm internal side length. Behind each piston is a rubber diaphragm sandwiched between the piston and an outer plate fixed to the frame (see Fig. 2). Each diaphragm is secured by an array of 8-mm diameter bolts connecting the outer plate to the frame. The bolts are designed to withstand the tensile force resulting from a maximum working piston pressure of 1.5 MPa. The number of bolts was also chosen to prevent any leakage of the fluid (water or silicon oil) used to pressurize the piston.

To allow all the pistons to move freely without constraining each other, the length of each piston is limited to 215 mm (i.e., 17.5 mm smaller than the chamber size from each side). Each piston is attached to a cylindrical guide (Fig. 2) that moves through a central hole (provided with an O-ring) drilled into the outer plate. The movement of each piston inside the chamber is limited to 10 mm when the inner face of the lip attached to the guide comes in contact with the outer plate. For an initial sample length of 250 mm, this means that the maximum rectilinear strain in any direction is 8 % (when each two faces are allowed to move freely simultaneously).

Each of the six pistons is provided with an 8-mm diameter hole covered with a sintered disk to allow drainage to a volume change measuring device. The rectilinear deformation of the soil on each side is measured via a potentiometer (Figs. 1 and 2) fixed to a bracket, so that the relative displacement between the piston and the fixed outer plate is obtained. Obviously, the total displacement in any direction is the algebraic sum of the measurement recorded by the two opposite potentiometers fixed to the faces of interest.

To lock any one of the pistons in place during a test, a special stainless steel "security" plate of 10-mm thickness is used. This plate is fixed to the piston through the cylindrical guide via two bolts. Two other bolts are fixed to the outer plate and pass through two holes drilled into the security plate. Two nuts running over these bolts are tightened to fix the security plate in position, and hence, the piston. This arrangement prevents the piston from moving outwards, thereby preventing the sample from expanding. This procedure is essential in K_o testing. Another two jack screws are used to ease pulling the piston out after test completion (Fig. 1).

Wave Velocity Measuring System

To enable measurement of V_s and V_p in a soil sample inside the chamber of the true triaxial apparatus, it was decided to adopt a system that allows the wave transducers to access the sample externally. To this end, a 25-mm diameter hole was drilled inside the outer cylindrical guide through to the piston. A stainless steel plate of 40-mm diameter and 3-mm thickness was then used to cover the hole at the interface between the piston and the sample, with an O-ring in between to prevent any leakage of water when testing saturated soils (see Cross Section A-A of Fig. 2).

Special normal incidence, flat shear, and compression wave transducers (Fig. 3) were manufactured at UWA from small piezoceramic plates. In the manufacturing process, the plates are bonded to a circular disk, which is glued to a stainless steel cylinder. Another circular disk is glued to the other end of the cylinder, and a 3-mm central hole is made for wiring. A schematic diagram showing details of the transducer is provided in Fig. 4.

The process of manufacturing a piezoelectric material involves application of a strong d-c electric field, which imparts permanent polarization to the crystals constituting the material. The piezoelectric material is then cut carefully into small sections, depending on the required application. In this paper, piezoceramic plates were cut out of rods manufactured by APC Ltd. (APC 855). The shear deformation of the piezoceramic element was obtained by positioning the crystal so that the direction of its permanent polarization is perpendicular to the applied electric field, and the axis of the casing housing (or the wave propagation direction) is made also perpendicular to the polarization direction. This is shown schematically in Fig. 5*a* for the shear mode. Conversely, the compression transducer (Fig. 5*c*) is assembled such that the polarization direction of the piezoceramic crystal coincides with the wave propagation direction. Hence, a compression wave is generated where the soil

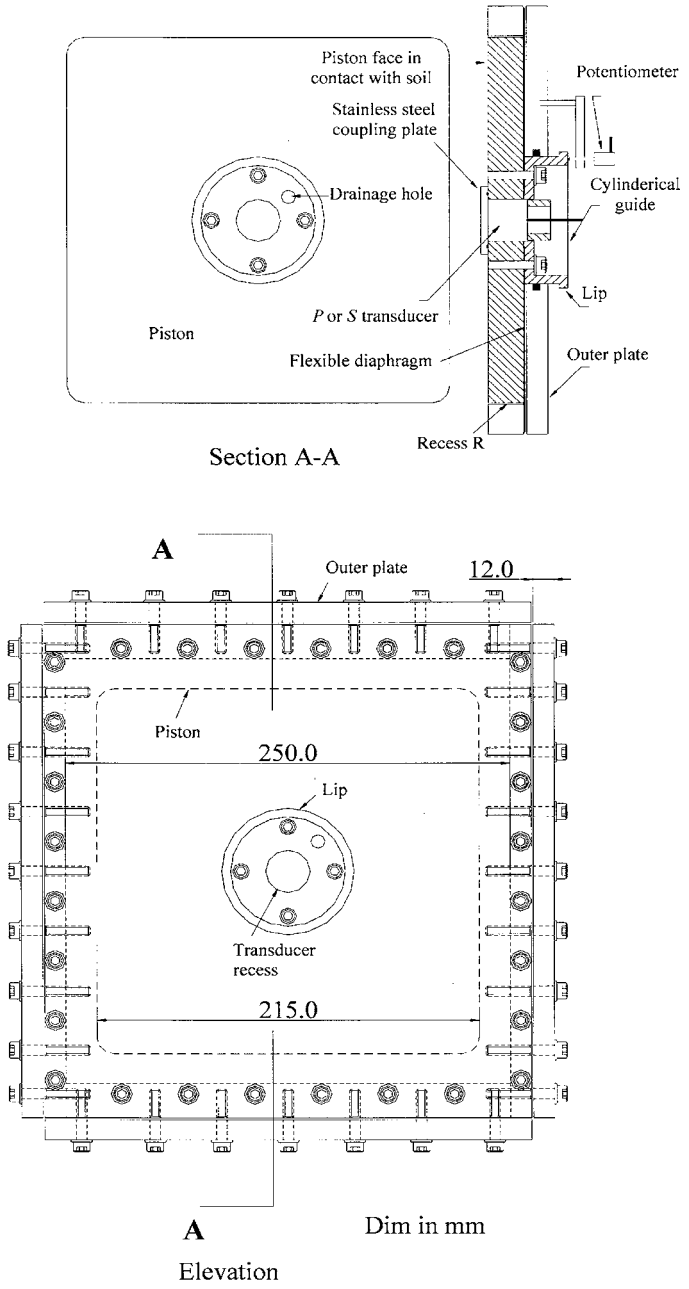

FIG. 2—*Elevation and section of the true triaxial apparatus.*

particles oscillate in the same direction of the wave propagation. Unlike the familiar bender elements (Dyvik and Madshus 1985), there is no difference between the transmitter and receiver using the technique described above. More details on the wave and compression transducers can be found in Ismail and Rammah (2004).

A function generator of the type Aiglmnet T15 was used to generate a single high-frequency (in the range 4–15 kHz) sine wave every 0.1 s. The generated signal was amplified to 220 V peak-to-peak before reaching the transmitter using a special voltage amplifier designed and manufactured at UWA. Received signals were also passed through a second voltage amplifier ($\times 100$) before being analyzed via a Pico oscilloscope. The traces of both the transmitted and received signals were downloaded to a PC via an RS-232 interface at a frequency of 0.5 MHz. Each reading was taken as the average of 64 stacked signals.

TABLE 1—*Verification of picking the far field during shear wave velocity measurement.*

V_s (m/s)	f_{output} (Hz)	λ (cm)	L (cm)	L/λ	Remarks
60	2 000	3.00	24.4	8.17	Very soft clay and loose sand
1000	15 000	6.67	24.4	3.67	Soft rock and strongly cemented soil

In these sorts of applications, near field effects (e.g., Sanchez-Salinero et al. 1986; Brignoli et al. 1996) are known to mask received signals and complicate the interpretation process. Brignoli et al. (1996) reported that near field effects can be avoided if the wave travel distance is at least twice the wave length (λ) of the output signal. The range of shear wave velocities expected to be measured for two extreme cases of geomaterials (i.e., very soft clay or loose sand and strongly cemented soil or soft rock) is listed in Table 1. Accordingly, the dimension $L = 250$ mm of the true triaxial device was carefully chosen to ensure that $L/\lambda \geq 2$ for a wide range of geomaterials.

One of the most crucial aspects in designing the wave velocity measuring system described here is to ensure that the received signal represents the wave that is truly propagating into the soil, and that no other (acoustically shorter) path was followed by the signal. This is particularly important here, because of: (i) the connectivity between the six outer faces of the apparatus and (ii) the wave transducers are not embedded into the tested soil sample, as in the case of large calibration chambers (for example, Belloti et al. 1996). This problem was overcome in the true triaxial device described by Stokoe et al. (1985) by acoustically insulating the connection between the transducers and surrounding metals using soft rubber. In fact, this problem is nonexistent in the apparatus described here, because the vibrating plate that is in contact with the soil (see recess R in Sec A-A, Fig. 2) is mounted on the piston, which moves freely inside the outer frame with a clearance of about 50 μm. Therefore, there is no closed loop that the signal can go through between the transducers other than through the soil itself. However, to confirm the absence of any cross paths of the waves generated by the wave transducers, an experiment was carried out in which each transducer was excited at one side of the (empty) apparatus and the response of the opposite one was monitored: no signal was received from this exercise.

Calibration of the Wave Velocity Measuring System

The wave velocity measuring system was calibrated against a cylindrical aluminum block, the shear and compression wave velocities of which are known to be 3130 m/s and 6320 m/s, respectively (Panametrics Catalogue 2003). The aluminum block had a diameter of 72 mm and length of 238 mm. The calibration was carried out (Fig. 6) by holding the block horizontally between two vertical pistons followed by applying a small pressure of only 5 kPa behind each piston. Both V_s and V_p were measured using the system described above and excellent agreement was found between the measured values and those reported above.

The ability of the system to capture stiffness isotropy of materials was also confirmed by filling the chamber with distilled water and measuring the compression wave velocity of the water (P_w) using different combinations of compression transducers along the three axes of the apparatus. Values of $P_w = 1472$ m/s, 1475 m/s, and 1485 m/s were measured, confirming the ability of the setup to both

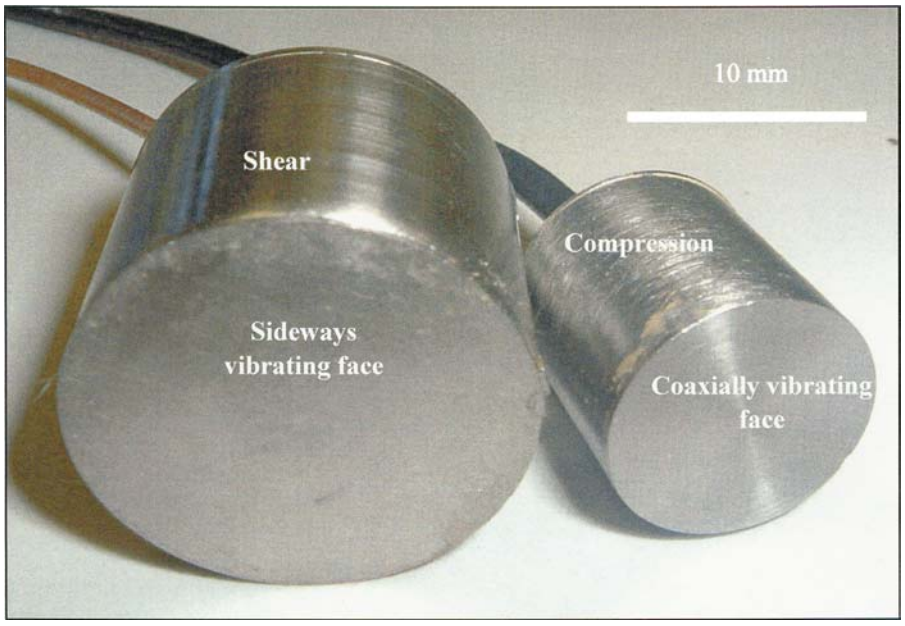

FIG. 3—*Photo of the shear and compression transducers manufactured at UWA.*

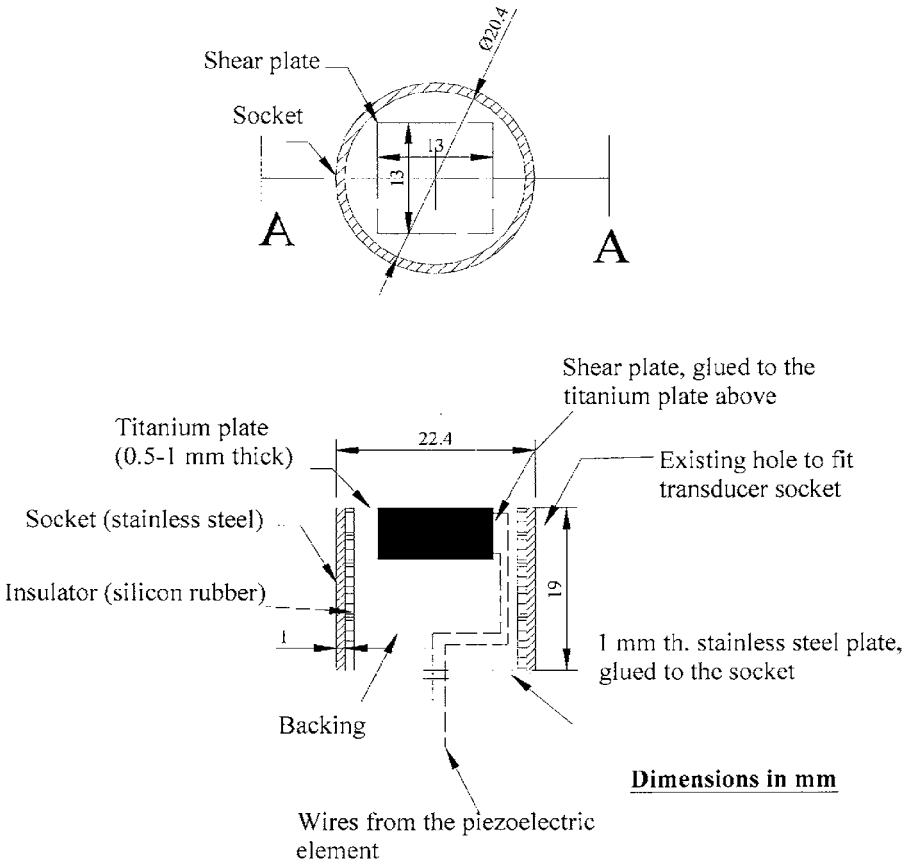

FIG. 4—*Details of assembly of shear or compression wave transducers (after Ismail and Rammah 2004).*

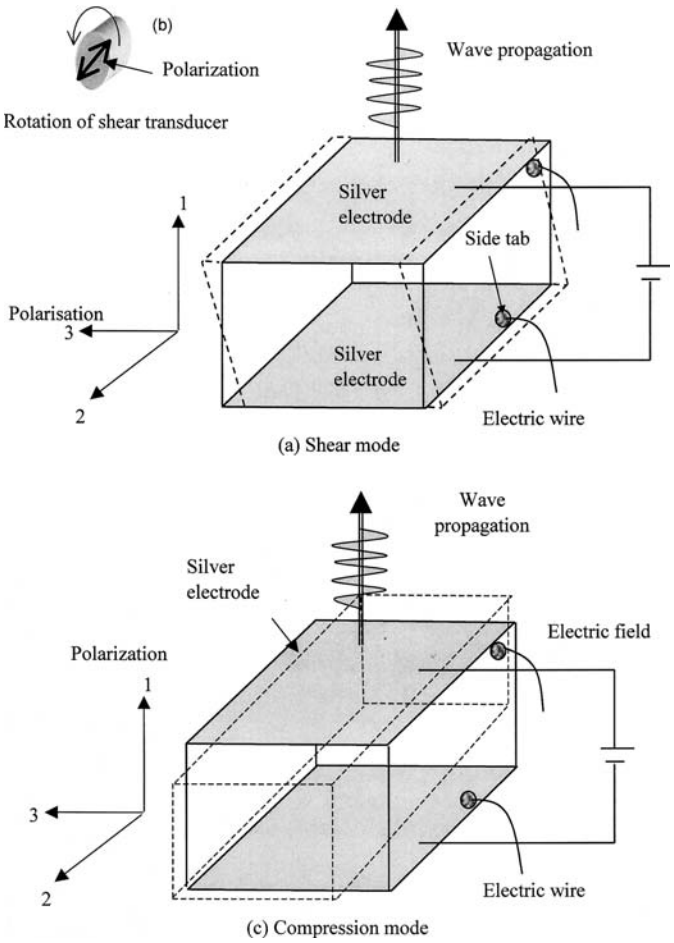

FIG. 5—*Shear and compression modes of wave propagation.*

capture the isotropic nature of the water and determine the velocity accurately ($P_w = 1480$ m/s at 20°C).

Advantages and Limitations of the New Triaxial Apparatus

The main advantages of the new apparatus can be summarized as follows:

1. The setup allows both drained and undrained tests to be carried out.
2. The setup is of the rigid type; hence, membrane penetration does not exist when coarse soil is tested.
3. Both uncemented and cemented samples can be tested.
4. The setup is ideal to test the influence of creep on stiffness under any general stress condition.
5. The horizontal stress can be accurately measured under 1-d compression conditions by connecting the pressure chamber behind the diaphragm to a back pressure unit set to zero volume change. This allows accurate measurement of K_o, as the stresses are measured as an average over the whole area of the piston. This method is more accurate than using a local stress cell.
6. Cyclic loading can be applied by programming the pressure regulators feeding the fluid chamber behind the diaphragm.
7. Both compression and shear wave transducers access the sample externally; therefore, they do not get affected by the stresses applied to the sample and they do not have to be water tight.
8. The compression and shear wave transducers are manufactured from thick piezoceramic crystals, which can take up to 600 V without depolarization. This feature allows the wave velocity to be measured in soft media that would otherwise attenuate the signal if low voltage is used (as in the case of bender elements).

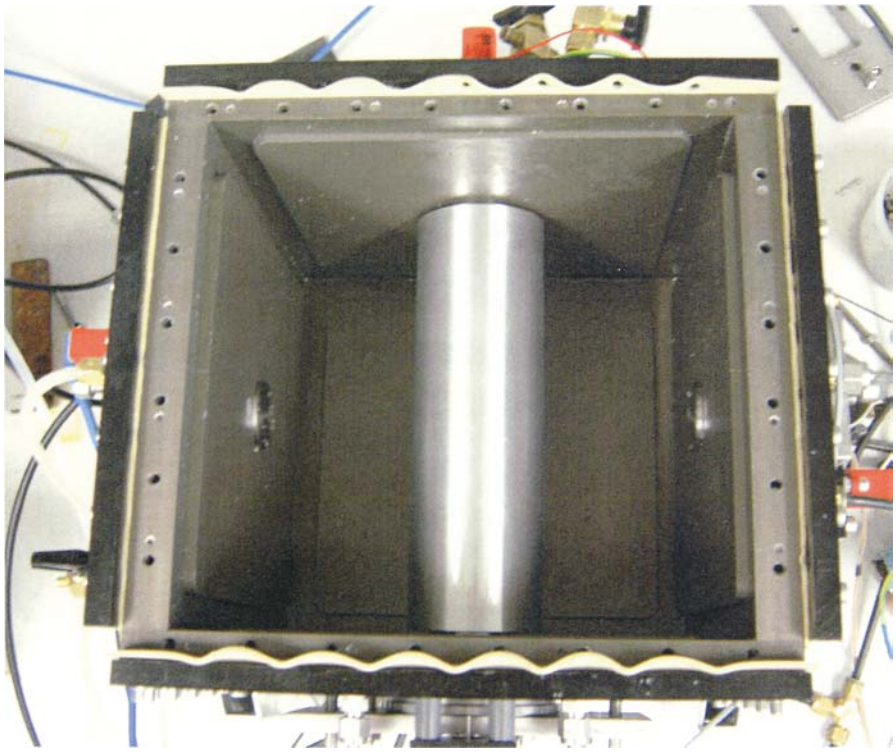

FIG. 6—*Calibration of the wave measuring system using an aluminum block.*

9. The shear wave transducers can be rotated (see icon of Fig. 5*b*), enabling, for example, $V_{s\text{-}h\theta}$ to be determined for a wave propagating horizontally with soil particles oscillating along a skew plane at an angle θ to the vertical. The angle θ may vary between 0° [for $V_{s\text{-}hv}$] and 90° [for $V_{s\text{-}hh}$]. This feature is extremely important in the course of determining the planes of anisotropy (Ismail et al. 2004), and hence, the relevant constitutive relationships to be developed. The measurement of either V_s or V_p can also be made along a skew wave propagation path between two perpendicular faces.

On the other hand, the setup in its current version has the following limitations:

1. The maximum rectilinear strain is limited to only 8 %.
2. The maximum normal stress that can be applied is 1.5 MPa.
3. The piston dimension is smaller than the side length of the chamber. This is envisaged to create some stress nonuniformity at the corners of the cubic chamber.
4. Friction exists at the interface between the walls and the tested soil; however, this can be significantly reduced by using a sandwich of latex rubber and silicon grease at the interface, as will be explained later.

Notation Used for Velocities and Stresses

Figure 7 illustrates the typical polarization and propagation directions used to generate and detect both shear and compression wave velocities in a cubic sample. The following notations are used later in the analysis section:

- V_{px} is the velocity of a compression wave propagating in the horizontal direction along the X axis with particle oscillation in the same direction;
- V_{py} is the velocity of a compression wave propagating in the horizontal direction along the Y axis with particle oscillation in the same direction;
- V_{pz} is the velocity of a compression wave propagating in the vertical direction along the Z axis, with particle oscillation in the same direction;
- $V_{s\text{-}xz}$ is a velocity of shear wave propagating in the horizontal direction along the X axis, with particle oscillating in the Z (i.e., vertical) direction;
- $V_{s\text{-}yx}$ is a velocity of shear wave propagating in the horizontal direction along the Y axis, with particle oscillating horizontally along the X axis.

Sample Preparation

Obviously, the sample preparation technique depends on the type of soil (i.e., coarse grained or fine-grained), and whether the sample is dry or saturated, and cemented or not. In all cases, the first step in the sample preparation is to remove the top piston, so that the chamber can be accessed. To reduce the friction between the soil and inside walls, about a 1.0-mm layer of silicon grease is first applied to the inner surfaces of the chamber. A layer of liquid latex is then brushed on top of the silicon grease and left to cure partially for 10–15 min. Latex application is repeated twice more and left to cure for several hours to form the first layer. To accelerate rubber vulcanization, hot air may be circulated inside the chamber using a hot air gun. After complete curing of the first layer, a second layer may be made with another 1.0 mm silicon grease in between. This arrangement results in alternating layers of grease and latex membrane similar to that used in lubricated ends in the conventional triaxial apparatus. In addition to its function in reducing the friction (the interface friction angle was reduced to about 2°), the latex sandwich also protects the aluminum walls of the apparatus. It should be noted, however, that the stainless steel plate that couples with the wave transducer must be exposed before placing the soil; otherwise, the latex rubber may attenuate the signals, particularly in shear (see Fig. 8)

Uncemented dry or saturated sand can be prepared by raining the dry sand from a constant height using a sand hopper to achieve the required density. Also, the sand may be poured manually from

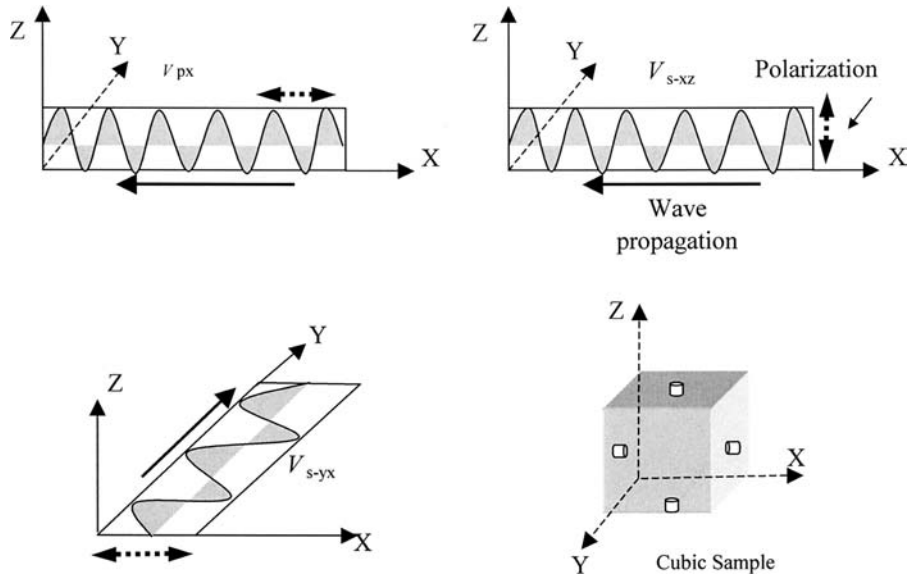

FIG. 7—*Shear and compression wave velocities measured in this study.*

FIG. 8—*The triaxial cell coated with latex rubber.*

a funnel that can be steadily raised towards the top surface. Alternatively, dry sand samples can be vibrated for densification before securing the top cover. Saturation of coarse soils can be achieved by flushing water though the sample and application of back pressure.

Samples of cemented sands can be prepared by moist compaction of a mixture of the sand and cement (e.g., Portland cement, gypsum, or casting resin). Alternatively, water can be flushed through a dry mixture of sand and cement (Portland cement and gypsum) prepared to a certain density inside the chamber. Aqueous chemical solutions can also be flushed or injected into a dry or saturated sand sample inside the chamber, and left to cure.

Clay samples are prepared by first consolidating them outside the setup to the required pressure. A cube about 2 mm smaller than the size of the triaxial chamber is then cut from the larger consolidated sample, and placed into the apparatus, ready for application of the required final consolidation stresses.

Description of Tested Soil

The capabilities of the new apparatus were investigated by carrying out a comprehensive testing program (described later) on a sample of silica sand. This is a rounded uniform blast sand of an average diameter (D_{50}) of 0.47 mm. Some physical properties of the sand are listed in Table 2. This sand was deliberately selected because of its bulky, rounded particles and absence of apparent structure anisotropy, as can be seen from the micrograph of Fig. 9.

TABLE 2—*Physical properties of the tested silica sand.*

G_s	D_{10} (mm)	D_{50} (mm)	% Fines	e_{max}	e_{min}	$CaCO_3$ (%)
2.64	0.320	0.47	0.30	0.755	0.520	0

Testing Program and Procedures

The testing program aimed at measuring V_s and V_p in various directions under four different stress conditions:

1. K_o stress condition,
2. Isotropic stress condition,
3. Where two principal stresses were kept constant and the third was increased steadily,
4. Under a general stress path in which the mean effective stress (p') was kept constant.

Only results from Phases 2 and 3 are presented in this paper. In Phase 2, each of the three principal stresses was increased simultaneously in increments of 18 kPa until a final stress of 148 kPa was reached. The aim of Phase 3 was to determine the dependency of the wave velocities on the individual components of the principal stresses (σ'_x, σ'_y, and σ'_z). This was carried out by holding each two stress component constant at 18 kPa and increasing the third over increments of 18 kPa to a maximum stress value of 148 kPa. In both cases, each of the wave velocities, V_{px}, V_{pz}, V_{py}, $V_{s\text{-}xz}$, and $V_{s\text{-}yx}$ was measured at each stress level.

Three pressure regulators are required to run a test, ideally each being computer-controlled. Each regulator is connected to each of two opposite faces of the apparatus. This arrangement not only guarantees equal pressure, but it also reduces the friction between the soil and the chamber walls due to the symmetry effect, which should produce zero shear stresses at the middle planes (see Fig. 10).

Analysis and Discussion of Results

Wave Velocities under Isotropic Conditions

Figure 11 shows typical traces of transmitted and received signals obtained during the isotropic stress test for the compression wave

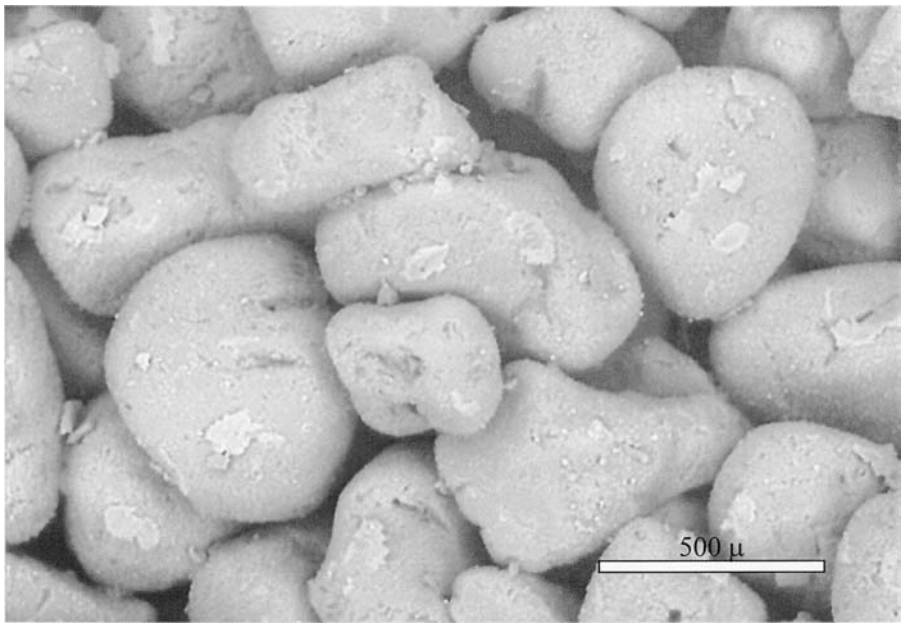

FIG. 9—*Micrograph of tested silica sand from scanning electron microscope.*

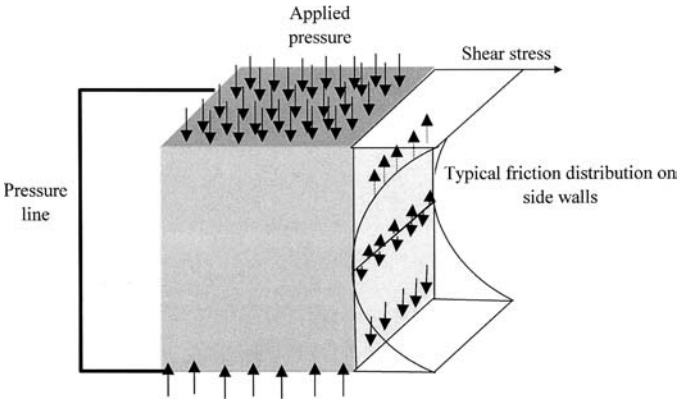

FIG. 10—*Influence of symmetry on shear stresses at the interface between a tested sample and apparatus walls.*

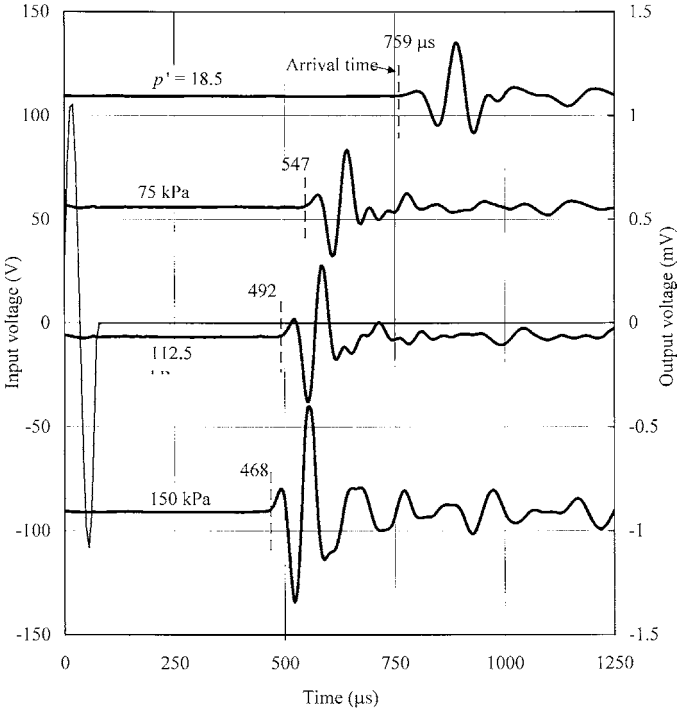

FIG. 11—*Traces of transmitted and received signals of V_{pz} under isotropic stress condition.*

velocity in the vertical direction (i.e., V_{pz}). Arrival time was chosen to be the point of first deflection of the output signal. The arrival time was found to be independent of the frequency of the input signal (a single-cycle sine wave) within the range of frequency used in this study (4–15 kHz). The input frequency was chosen to produce the highest output amplitude.

Figure 12 presents the variation of the velocities V_{px}, V_{pz}, V_{py}, $V_{s\text{-}xz}$, and $V_{s\text{-}yx}$ with the variation in isotropic stress (p'). Three main observations can be made from this figure. First, the compression wave velocity in all three directions (i.e., V_{px}, V_{pz}, V_{py}) are almost identical, reflecting the absence of any initial fabric (or structural) anisotropy, as indicated previously from the micrograph shown in Fig. 9. Each of V_{px}, V_{pz}, and V_{py} increases with p' according to a power law, with exponent $n = 0.24$. This value lies within the range of 0.20–0.25 reported for silica sands by other investigators (e.g., Hardin and Drnevich 1972; Belloti et al. 1996; Stokoe et al. 1985). Second, the shear wave velocities in the horizontal ($V_{s\text{-}yx}$) and vertical ($V_{s\text{-}xz}$) planes are also identical, another indication of the isotropy of the sand structure. Both $V_{s\text{-}yx}$ and $V_{s\text{-}xz}$ also increase with p' according to a power law. However, it is well established (e.g., Roesler 1979; Bellotti et al. 1996) that this increase is not due to the increase in p' *per se*, but is a result of the increasing normal stresses within the shearing plane, as will be shown later. Third, overconsolidation of the sand has very negligible effect on the small-strain stiffness. This is confirmed by comparing V_{pz} during loading (open circles of Fig. 12) and unloading (solid circles); this observation is typical for all other velocities in the figure.

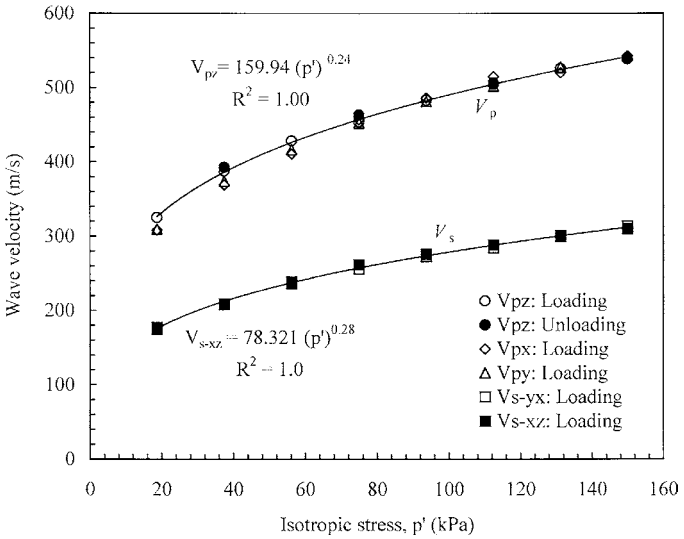

FIG. 12—*Influence of isotropic stress on compression and shear wave velocities.*

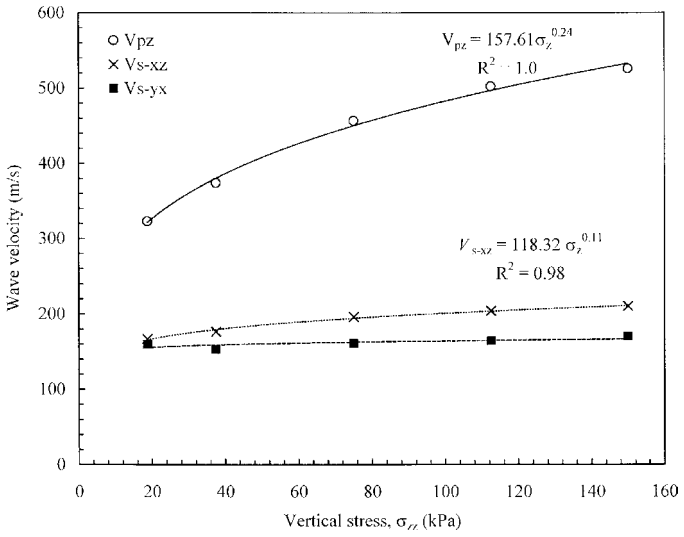

FIG. 13—*Influence of varying* $\sigma'_x(\sigma'_y = \sigma'_z = constant = 18\,kPa)$ *on* V_{px}, $V_{s\text{-}xz}$, $V_{s\text{-}yx}$.

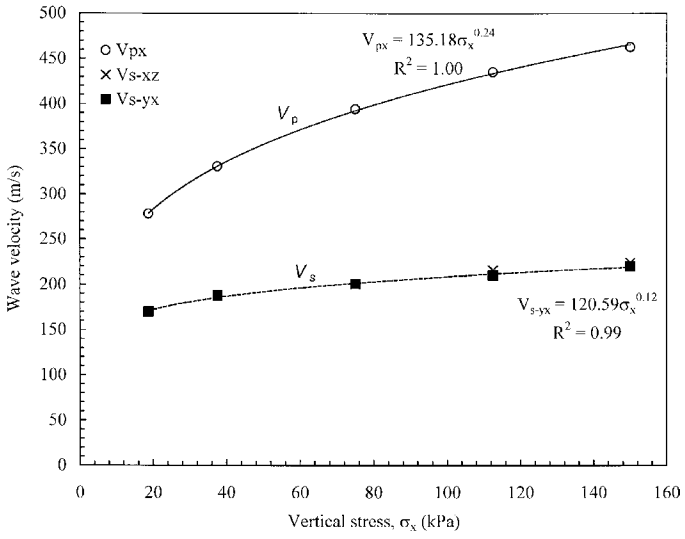

FIG. 14—*Influence of varying* $\sigma'_y(\sigma'_x = \sigma'_z = constant = 18\,kPa)$ *on* V_{px}, $V_{s\text{-}xz}$, $V_{s\text{-}yx}$.

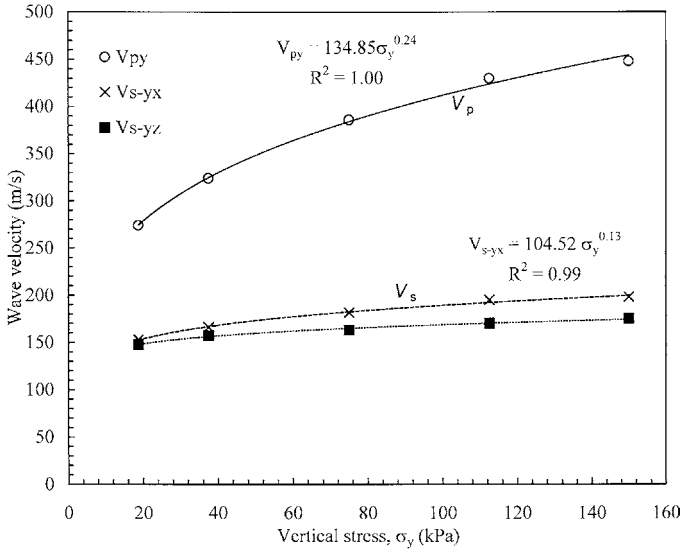

FIG. 15—*Influence of varying* $\sigma'_z(\sigma'_x = \sigma'_y = constant = 18\,kPa)$ *on* V_{px}, $V_{s\text{-}xz}$, $V_{s\text{-}yx}$.

TABLE 3—*Constants of the power relationships from variation of one stress component.*

	σ_x		σ_y		σ_z		
Velocity	n*	R^2	n	R^2	N	R^2	Remarks
V_{px}	0.24	1.0	Independent		0.01	0.69	Each stress component
V_{py}	Independent		0.24	1.0	0.04	0.35	was varied from 18 kPa
V_{pz}	Independent		Independent		0.24	1.0	to 148 kPa; the other two
$V_{s\text{-}xy}$	0.12	0.99	0.13	0.99	Independent		were kept constant at
$V_{s\text{-}xz}$	0.11	0.98	Independent		0.13	0.98	18 Pa

* n is the exponent in the form $V_i = B(\sigma_i)^n$, where V is the compression or shear wave velocity.

Variation of Wave Velocities with Principal Stresses

Results of the series of testing in which only one principal stress was increased are shown in Figs. 13, 14, and 15. It is clear that each of V_{px}, V_{py}, and V_{pz} is influenced only by the stress component in the direction of the wave propagation (i.e., σ'_x, σ'_y, and σ'_z, respectively). On the other hand, $V_{s\text{-}xz}$ is influenced by only σ'_x and σ'_z, while $V_{s\text{-}yx}$ is influenced by only σ'_y and σ'_x. These results confirm the capability of the new device in capturing the evolution of small-strain stiffness with stresses, as reported in the literature. Table 3 summarizes the exponents of the power relationships through which each of the wave velocities changes with the corresponding stress.

Concluding Remarks

This paper presented a new true triaxial device capable of measuring the shear and compression wave velocity in any predetermined direction. The main advantage of the device is the ability to make the wave velocity measurements external to the sample. In-house manufactured compression and shear wave transducers are described. Their main advantage is that these transducers are flat and they do no have to penetrate the soil, as in the case of bender elements.

The new apparatus was used to investigate the characteristics of seismic waves propagating through silica sand under isotropic and anisotropic stress conditions. The apparatus produced results that are consistent with those reported in the literature for similar sands.

Acknowledgements

The work in this paper forms part of the activities of the Centre for Offshore Foundation Systems (COFS), established and supported under the Australian Research Council's Research Centres Program.

References

Bellotti, M., Jamiolkowski, M., Presti, D. C. F. L., and O'Neill, D. A., 1996, "Anisotropy of Small Strain Stiffness in Ticino Sand," *Géotechnique*, Vol. 46, No. 1, pp. 115–131.

Brignoli, E. G. M., Gotti, M., and Stokoe, K. H. I., 1996, "Measurement of Shear Waves in Laboratory Specimens by Means of Piezoelectric Transducers," *Geotechnical Testing Journal*, Vol. 19, No. 4, pp. 384–397.

Dyvik, R. and Madshus, C., 1985, "Lab Measurements of G_{max} Using Bender Elements," *Advances in the Art of Testing Soils Under Cyclic Conditions*, Conference, Detroit, MI, Geotechnical Engineering Division, *ASCE*, New York.

Dyvik, R. and Olsen, T. S., 1989, "G_{max} Measured in Oedometer and DSS Tests Using Bender Elements," *Proceedings, 12th International Conference on Soil Mechanics and Foundation Engineering,* Rio de Janeiro, Vol. 1, pp. 39–42.

Hardin, B. O. and Drnevich, V. P., 1972, "Shear Modulus and Damping in Soils: Measurements and Parameter Effects," *ASCE Journal of Soil Mechanics and Foundation Division*, Vol. 98, pp. 603–624.

http://www.panametricsndt.com/ndt/our_products/products/ndt_transducers/index.htm (Accessed 25/2/04).

Ismail, M. A., Ferierra, C., and Fahey, M., 2004, "Influence of Cement Type on G_o of a Carbonate Sand," *A Forthcoming Skempton Symposium,* Vol. 1, pp. 464–472.

Ismail, M. A. and Rammah, K., 2004, "Shear-Plate Transducer as an Alternative to Bender Elements," (submitted to *Géotechnique*).

Nakamura, Y., Kuwano, J., and Hashimoto, S., 1999, "Small-Staring Stiffness and Creep of Toyoura Sand Measured by a Hollow Cylinder Apparatus," *Proceedings, 2nd International Conference on Pre-Failure Deformation Characteristics of Geomaterials*, Torino, Italy, Vol. 1, pp. 141–148, Balkema, Rotterdam.

Panametrics On-Line Catalogue (2004).

Pennington, D. S., Nash, D. F. T., and Lings, M., 2001, "Horizontally Mounted Bender Element for Measuring Anisotropic Shear Moduli in Triaxial Clay Specimens," *Geotechnical Testing Journal*, Vol. 24, No. 2, pp. 133–144.

Roesler, S. K., 1979, "Anisotropic Shear Modulus Due to Stress Anisotropy," *ASCE Journal of Geotechnical Engineering*, Vol. 105, No. GT7, pp. 871–880.

Saada, A., 1988, "Hollow Cylinder Torsional Devices, Their Advantages and Limitations," *ASTM STP 977*, ASTM International, West Conshohocken, PA, pp. 766–795.

Sanchez-Salinero, I., Roesset, J. M., and Stokoe, K. H. I., 1986, "Analytical Studies of Body Wave Propagation and Attenuation," *Geotechnical Engineering*, GR86-15, University of Texas at Austin.

Santamarina, J. C. and Cascante, G., 1996, "Stress Anisotropy and Wave Propagation: a Micromechanical View," *Canadian Geotechnical Journal*, Vol. 33, pp. 770–782.

Stokoe, K. H. I., Lee, S. H. H., and Knox, D. P., 1985, "Shear Moduli Measurements Under True Triaxial Stresses," *Advances in the Art of Testing Soils Under Cyclic Conditions*, ASCE, Detroit, MI, pp. 166–185.

Yu, P. and Richart, F. E., 1984, "Stress Ratio Effects on Shear Modulus of Dry Sands," *ASCE Journal of Geotechnical Engineering*, Vol. 110, No. 3, pp. 331–345.

Zeng, X. and Ni., B., 1999, "Stress-Induced Anisotropic G_{max} of Sands and its Measurement," *ASCE Journal of Geotechnical and Geoenvironmental Engineering*, Vol. 125, No. 9, pp. 741–749.